Research Article *Energy, Environment and Storage* (2025) 05-02:58-66

Energy, Environment and Storage

Journal Homepage: www.enenstrg.com

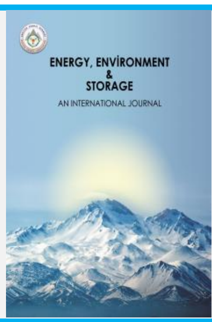

Drought Prediction Based on Global Atmospheric Circulation Indices Using Artificial Neural Networks: A Case for City of Kayseri, Türkiye

Fadime KILIÇ[1], Ali Ümran KÖMÜŞCÜ[2], Filiz DADAŞER-ÇELİK[3*,]

[1] *Graduate School of Natural and Applied Sciences, Erciyes University, Kayseri, Türkiye, ORCID: https://orcid.org/0009-0009-7743-8098*

[2] *Dept. of Geography, Ankara Hacı Bayram Veli University, Ankara, Türkiye, ORCID: https://orcid.org/0000-0001-9930-2479*

[3] *Dept. of Environmental Engineering, Erciyes University, Kayseri, Türkiye, ORCID: https://orcid.org/0000-0003-3623-7723*

ABSTRACT. Drought is a complex natural phenomenon resulting from prolonged periods of below-average precipitation. Its gradual development over large areas makes it challenging to accurately determine its onset, duration, and overall impact. This study developed an artificial neural network (ANN) method-based model to predict the standard precipitation index (SPI), an index commonly used to determine drought severity. SPI12, which reflects a meteorological drought indicator to monitor precipitation anomalies over 12-month accumulation periods, was estimated based on the artificial neural network (ANN) method using monthly precipitation data recorded in the 1980-2015 period for Kayseri. The North Atlantic Oscillation Index (NAOI), Mediterranean Oscillation Index (MOI), and Arctic Oscillation Index (AOI), which represent large-scale global cycles, were used as input variables in the models. A multilayer perceptron-type ANN model with a single hidden layer was chosen. The model training used 70% of the data and a scaled conjugate gradient backpropagation algorithm. The remaining 30% of the data were used for model testing and control. The activation functions of the ANN model and the number of neurons in the hidden layer were determined using the trial-and-error method. The performances of the models were evaluated using the mean Nash-Sutcliffe coefficient of efficiency (NSE), root mean square error (RMSE), and coefficient of determination (R^2) of agreement between the estimated and observed SPI12 values. This study demonstrated that drought conditions can be successfully predicted 3, 6, and 12 months in advance using indices reflecting large-scale global climate anomalies.

Keywords: Drought, Drought Prediction, Artificial Neural Networks, Precipitation, Standard Precipitation Index

Article History: Received:13.04.2025; Revised: 06.05.2025; Accepted:08.05.2025; Available Online: 11.05.2025

Doi: https://doi.org/10.52924/SNRZ2925

1. INTRODUCTION

In recent years, due to changing climate characteristics, rapid development of the energy, industry, and agriculture sectors, and population growth, water demand has been steadily increasing, and water shortages are becoming more frequent. The frequency and severity of drought events are changing in many regions of the world. Understanding these changes and predicting future conditions are critical for preventing climate-related disasters.

Drought is a disaster that occurs when precipitation falls below normal levels for many years, causing the deterioration of the hydrological and ecological balance. Predicting the location, time, and duration of a drought event is difficult. Drought differs from other natural phenomena in the sense that it starts very slowly, develops over months or even years, and affects vast areas. It is also challenging to determine the beginning, end, effects, and consequences of droughts.

Various indices have been developed to characterize and monitor drought events. Each of these indices captures different aspects of drought, depending on data availability and the type of drought being studied [1]. Among these, the Standardized Precipitation Index (SPI) is one of the most widely used because of its simplicity, applicability over multiple timescales, and calculability based only on precipitation data.

In this study, we aimed to develop models for predicting drought events characterized by SPI values for Kayseri (Türkiye). We used Artificial Neural Networks (ANN), a machine learning technique that is widely used for

*Corresponding author: fdadaser@erciyes.edu.tr

predicting hydrologic and climatic variables. The input variables for the prediction models include large-scale global oscillation indices representing atmospheric circulation patterns, such as the North Atlantic Oscillation Index (NAOI), Mediterranean Oscillation Index (MOI), and Arctic Oscillation Index (AOI). Prediction models were developed to forecast the SPI12 value, which is the SPI value calculated based on 12-month data. Standard statistical performance metrics were used to evaluate the performances of the developed models.

2. MATERIALS AND METHODS

2.1 Data Used

This study used monthly precipitation data from 1980 to 2015 recorded at the meteorology station number 17196, located in Kayseri. The precipitation data then were used to calculate the SPI values. The SPI [2] was developed to normalize the statistical distribution of precipitation data to eliminate the differences resulting from nonstandard distributions. To calculate the SPI, precipitation data are first fitted to a gamma distribution. The gamma distribution is preferred because precipitation data usually take positive values and have an asymmetric distribution. This fitted gamma distribution was then transformed into a normal distribution using an equal probability transformation. After transformation to a normal distribution, the SPI is expressed as a z-score with zero mean and unit standard deviation. SPI values above zero indicate above-average precipitation, that is, wet periods, whereas SPI values below zero reflect below-average precipitation, that is, dry periods. The SPI allows meteorological drought analysis at different time scales (3, 6, 12, 24, and 48 months). Because the precipitation deficit gradually and variably affects different water resources (e.g., streamflow and groundwater), multiple SPI periods can be used to reflect the changes in different water properties.

Studies conducted in Türkiye have shown that analyzing historical precipitation data, along with large-scale global oscillation indices, is crucial for generating future climate scenarios and predicting drought events [3, 4, 5, 6, 7, 8, 9, 10]. In this study, drought prediction was performed based on SPI12 data and large-scale oscillation indices. The 12-month Standardized Precipitation Index (SPI12) is a meteorological drought indicator that is commonly used to monitor precipitation anomalies over 12-month accumulation periods. It is considered to be a proxy indicator for medium-term hydrological impacts, such as reduced stream flow and reservoir storage.

To describe large-scale atmospheric events, the NAOI, AOI, and MOI, which were previously identified as the most influential indices of precipitation in Türkiye by Dadaser-Celik et al. [11] were considered. The NAOI can be defined as the normalized pressure difference between a station in the Azores and a station in Iceland. The AOI was calculated by reflecting the daily 1000mb height anomalies of the polar oscillation in the poleward direction by 20°K on the loading pattern. The MOI was calculated as the normalized pressure difference between Algiers (36.4°N, 3.1°E) and Cairo (30.1°N, 31.4°E) (MOI1), or between the Northern Border of Gibraltar (36.1°N, 5.3°W) and Israel (32.0°N, 34.5°E) Lod Airport (MOI2). Because MOI1 and MOI2 show similar effects, only the MOI1 index was considered in this study. The time series containing the index data was obtained from the UK Climate Research Unit and the US Climate Prediction Center.

2.2 Model Setup

The model used SPI12 as the output (dependent variable), whereas the inputs (independent variables) included SPI12, NAOI, AOI, and MOI1 values from the preceding 3, 6, and 12 months (Table 1). In other words, the model inputs consisted of historical values of SPI and climate indices (NAOI, AOI, and MOI1) to predict future SPI12 conditions.

A multi-layer perceptron ANN model with a single hidden layer was selected. The model training used 70% of the data and a scaled conjugate gradient backpropagation algorithm. The remaining 15% of the data was used for testing, and the final 15% was used for validation. The data used for the training, testing, and validation were randomly selected. The activation functions of the hidden layer (hyperbolic tangent or sigmoid (S-shaped)) and the number of neurons in the hidden layer were determined using a trial-and-error method. Similarly, the activation functions of the output layer (identity, softmax, hyperbolic tangent, or sigmoid) were selected through trial and error. Additionally, models were run using activation functions with 1–50 neurons in the hidden layer, and the configuration that produced the least error was selected for the study.

The performances of the models were evaluated by calculating the Nash-Sutcliffe efficiency (NSE) coefficient, Root Mean Square Error (RMSE), and Coefficient of Determination (R^2). The NSE coefficient typically ranges between 0 and 1, with values closer to 1 indicating that the model performance has acceptable accuracy. An NSE value of 1 and/or close to 1 signifies that the success of the analysis is high [12]. The R^2 values change between 0 and 1, and values closer to 1 indicate higher performance. For the RMSE, values closer to zero were preferable.

Copyright © and. Published by Erciyes Energy Association

Table 1. Models Inputs and Outputs

Model No	Models Used in the Study
1	$SPI_{t+1} = f(SPI_{(t)}, SPI_{(t-1)}, SPI_{(t-2)}, SPI_{(t-3)})$
2	$SPI_{t+1} = f(SPI_{(t)}, SPI_{(t-1)}, SPI_{(t-2)}, SPI_{(t-3)}, NAO_{(t-1)}, NAO_{(t-2)}, NAO_{(t-3)})$
3	$SPI_{t+1} = f(SPI_{(t)}, SPI_{(t-1)}, SPI_{(t-2)}, SPI_{(t-3)}, AO_{(t-1)}, AO_{(t-2)}, AO_{(t-3)})$
4	$SPI_{t+1} = f(SPI_{(t)}, SPI_{(t-1)}, SPI_{(t-2)}, SPI_{(t-3)}, MOI_{(t-1)}, MOI_{(t-2)}, MOI_{(t-3)})$
5	$SPI_{t+1} = f(SPI_{(t)}, SPI_{(t-1)}, SPI_{(t-2)}, SPI_{(t-3)}, NAO_{(t-1)}, NAO_{(t-2)}, NAO_{(t-3)}, AO_{(t-1)}, AO_{(t-2)}, AO_{(t-3)})$
6	$SPI_{t+1} = f(SPI_{(t)}, SPI_{(t-1)}, SPI_{(t-2)}, SPI_{(t-3)}, NAO_{(t-1)}, NAO_{(t-2)}, NAO_{(t-3)}, AO_{(t-1)}, AO_{(t-2)}, AO_{(t-3)}, MOI_{(t-1)}, MOI_{(t-2)}, MOI_{(t-3)})$
7	$SPI_{t+1} = f(SPI_{(t)}, SPI_{(t-1)}, SPI_{(t-2)}, SPI_{(t-3)}, SPI_{(t-4)}, SPI_{(t-5)}, SPI_{(t-6)})$
8	$SPI_{t+1} = f(SPI_{(t)}, SPI_{(t-1)}, SPI_{(t-2)}, SPI_{(t-3)}, SPI_{(t-4)}, SPI_{(t-5)}, SPI_{(t-6)}), NAO_{(t-1)}, NAO_{(t-2)}, NAO_{(t-3)}, NAO_{(t-4)}, NAO_{(t-5)}, NAO_{(t-6)})$
9	$SPI_{t+1} = f(SPI_{(t)}, SPI_{(t-1)}, SPI_{(t-2)}, SPI_{(t-3)}, SPI_{(t-4)}, SPI_{(t-5)}, SPI_{(t-6)}, AO_{(t-1)}, AO_{(t-2)}, AO_{(t-3)}, AO_{(t-4)}, AO_{(t-5)}, AO_{(t-6)})$
10	$SPI_{t+1} = f(SPI_{(t)}, SPI_{(t-1)}, SPI_{(t-2)}, SPI_{(t-3)}, SPI_{(t-4)}, SPI_{(t-5)}, SPI_{(t-6)}, MOI_{(t-1)}, MOI_{(t-2)}, MOI_{(t-3)}, MOI_{(t-4)}, MOI_{(t-5)}, MOI_{(t-6)})$
11	$SPI_{t+1} = f(SPI_{(t)}, SPI_{(t-1)}, SPI_{(t-2)}, SPI_{(t-3)}, SPI_{(t-4)}, SPI_{(t-5)}, SPI_{(t-6)}, NAO_{(t-1)}, NAO_{(t-2)}, NAO_{(t-3)}, NAO_{(t-4)}, NAO_{(t-5)}, NAO_{(t-6)}, AO_{(t-1)}, AO_{(t-2)}, AO_{(t-3)}, AO_{(t-4)}, AO_{(t-5)}, AO_{(t-6)})$
12	$SPI_{t+1} = f((SPI_{(t)}, SPI_{(t-1)}, SPI_{(t-2)}, SPI_{(t-3)}, SPI_{(t-4)}, SPI_{(t-5)}, SPI_{(t-6)}, NAO_{(t-1)}, NAO_{(t-2)}, NAO_{(t-3)}, NAO_{(t-4)}, NAO_{(t-5)}, NAO_{(t-6)}, AO_{(t-1)}, AO_{(t-2)}, AO_{(t-3)}, AO_{(t-4)}, AO_{(t-5)}, AO_{(t-6)}, MOI_{(t-1)}, MOI_{(t-2)}, MOI_{(t-3)}, MOI_{(t-4)}, MOI_{(t-5)}, MOI_{(t-6)})$
13	$SPI_{t+1} = f(SPI_{(t)}, SPI_{(t-1)}, SPI_{(t-2)}, SPI_{(t-3)}, SPI_{(t-4)}, SPI_{(t-5)}, SPI_{(t-6)}, SPI_{(t-7)}, SPI_{(t-8)}, SPI_{(t-9)}, SPI_{(t-10)}, SPI_{(t-11)}, SPI_{(t-12)})$
14	$SPI_{t+1} = f(SPI_{(t)}, SPI_{(t-1)}, SPI_{(t-2)}, SPI_{(t-3)}, SPI_{(t-4)}, SPI_{(t-5)}, SPI_{(t-6)}, SPI_{(t-7)}, SPI_{(t-8)}, SPI_{(t-9)}, SPI_{(t-10)}, SPI_{(t-11)}, SPI_{(t-12)}, NAO_{(t-1)}, NAO_{(t-2)}, NAO_{(t-3)}, NAO_{(t-4)}, NAO_{(t-5)}, NAO_{(t-6)}, NAO_{(t-7)}, NAO_{(t-8)}, NAO_{(t-9)}, NAO_{(t-10)}, NAO_{(t-11)}, NAO_{(t-12)})$
15	$SPI_{t+1} = f(SPI_{(t)}, SPI_{(t-1)}, SPI_{(t-2)}, SPI_{(t-3)}, SPI_{(t-4)}, SPI_{(t-5)}, SPI_{(t-6)}, SPI_{(t-7)}, SPI_{(t-8)}, SPI_{(t-9)}, SPI_{(t-10)}, SPI_{(t-11)}, SPI_{(t-12)}, AO_{(t-1)}, AO_{(t-2)}, AO_{(t-3)}, AO_{(t-4)}, AO_{(t-5)}, AO_{(t-6)}, AO_{(t-7)}, AO_{(t-8)}, AO_{(t-9)}, AO_{(t-10)}, AO_{(t-11)}, AO_{(t-12)})$
16	$SPI_{t+1} = f(SPI_{(t)}, SPI_{(t-1)}, SPI_{(t-2)}, SPI_{(t-3)}, SPI_{(t-4)}, SPI_{(t-5)}, SPI_{(t-6)}, SPI_{(t-7)}, SPI_{(t-8)}, SPI_{(t-9)}, SPI_{(t-10)}, SPI_{(t-11)}, SPI_{(t-12)}, MOI_{(t-1)}, MOI_{(t-2)}, MOI_{(t-3)}, MOI_{(t-4)}, MOI_{(t-5)}, MOI_{(t-6)}, MOI_{(t-7)}, MOI_{(t-8)}, MOI_{(t-9)}, MOI_{(t-10)}, MOI_{(t-11)}, MOI_{(t-12)})$
17	$SPI_{t+1} = f(SPI_{(t)}, SPI_{(t-1)}, SPI_{(t-2)}, SPI_{(t-3)}, SPI_{(t-4)}, SPI_{(t-5)}, SPI_{(t-6)}, NAO_{(t-1)}, NAO_{(t-2)}, NAO_{(t-3)}, NAO_{(t-4)}, NAO_{(t-5)}, NAO_{(t-6)}, NAO_{(t-7)}, NAO_{(t-8)}, NAO_{(t-9)}, NAO_{(t-10)}, NAO_{(t-11)}, NAO_{(t-12)}, AO_{(t-1)}, AO_{(t-2)}, AO_{(t-3)}, AO_{(t-4)}, AO_{(t-5)}, AO_{(t-6)}, AO_{(t-7)}, AO_{(t-8)}, AO_{(t-9)}, AO_{(t-10)}, AO_{(t-11)}, AO_{(t-12)})$
18	$SPI_{t+1} = f(SPI_{(t)}, SPI_{(t-1)}, SPI_{(t-2)}, SPI_{(t-3)}, SPI_{(t-4)}, SPI_{(t-5)}, SPI_{(t-6)}, NAO_{(t-1)}, NAO_{(t-2)}, NAO_{(t-3)}, NAO_{(t-4)}, NAO_{(t-5)}, NAO_{(t-6)}, NAO_{(t-7)}, NAO_{(t-8)}, NAO_{(t-9)}, NAO_{(t-10)}, NAO_{(t-11)}, NAO_{(t-12)}, AO_{(t-1)}, AO_{(t-2)}, AO_{(t-3)}, AO_{(t-4)}, AO_{(t-5)}, AO_{(t-6)}, AO_{(t-7)}, AO_{(t-8)}, AO_{(t-9)}, AO_{(t-10)}, AO_{(t-11)}, AO_{(t-12)}, MOI_{(t-1)}, MOI_{(t-2)}, MOI_{(t-3)}, MOI_{(t-4)}, MOI_{(t-5)}, MOI_{(t-6)}, MOI_{(t-7)}, MOI_{(t-8)}, MOI_{(t-9)}, MOI_{(t-10)}, MOI_{(t-11)}, MOI_{(t-12)})$

3. RESULTS

3.1 Data Characteristics

The data used in this study consisted of precipitation data, SPI12 values calculated from the precipitation data, and large-scale circulation index data. The annual precipitation and the resulting SPI12 values for the 1980-2015 period for the city of Kayseri are shown in Figs. 1 and 2, respectively.

The average annual precipitation in Kayseri for the period 1980-2015 was calculated as 406 mm. The lowest precipitation in the study area occurred during summer, whereas the highest precipitation levels were observed in the spring and winter. The lowest annual average precipitation occurred in 2001, and the highest in 1988. August was the driest month, with an average monthly precipitation of 6.7 mm. The highest precipitation occurred in May, with an average of 57.5 mm.

The SPI12 values range from a minimum of -2.53 to a maximum of 2.72. Dry periods occurred in the years 1981, 1983, 1985, 1990, 1995, 2001, 2002, 2004, 2005, 2006, 2009, and 2014, while wet periods were observed in the years 1987, 1988, 1989, 1991, 1992, 1998, 1999, 2000, 2003, 2007, 2010, 2011, 2012, and 2015.

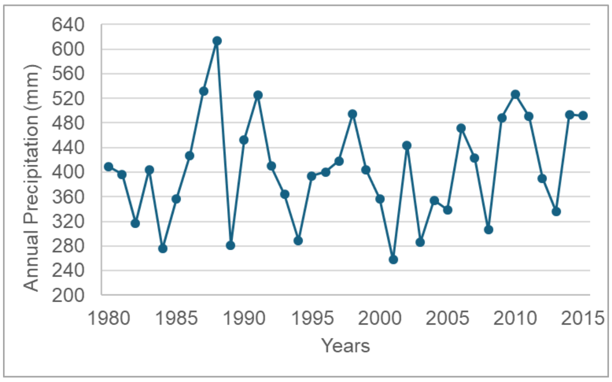

Fig. 1. Annual Precipitation between 1980 and 2015

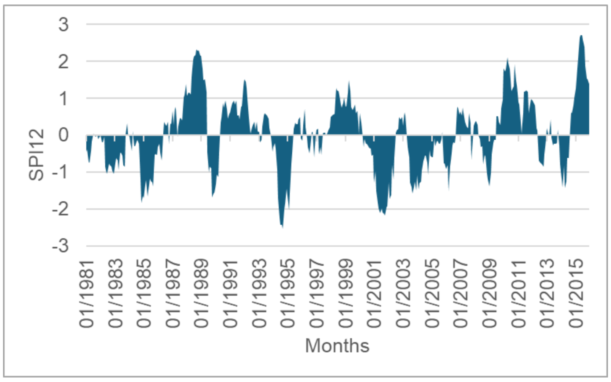

Fig. 2. SPI12 values for the 1981-2015 period

3.2 SPI12 Forecasting Using Data from the Past 3 Months

In the first part of the study, SPI12 values were predicted using the SPI12, NAOI, AOI, and MOI1 values from the past 3 months (Models 1 to 6 in Table 1). The results obtained from predicting SPI12 with different inputs are shown in Figs. 3 and 4. The calculated NSE, RMSE, and R^2 values are presented in Table 2. When data from the past three months were used (Models 1 to 6), Models 3 and 6 were the best-performing models. In Model 3, SPI12 values were predicted using the SPI12 and AOI values in the previous one, two, and three months. In Model-6, SPI12 values were predicted using SPI12, NAOI, AOI, and MOI1 values from the last 1, 2, and 3 months. The NSE, R2, and RMSE values in both models were 0.89, 0.89, and 0.33, respectively. The best model performance was obtained when the hyperbolic tangent was selected as the activation function in the hidden layer and the identity function was used in the output layer.

Table 2. SPI12 Prediction Performance Based on Past 3 Months' Data

Model No	TRAIN			TEST			VALIDATION			ALL		
	NSE	RMSE	R^2	NSE	RMSE	R^2	NSE	RMSE	R^2	NSE	RMSE	R^2
MODEL 1	0.91	0.34	0.88	0.91	0.19	0.82	0.90	0.17	0.90	0.88	0.34	0.89
MODEL 2	0.90	0.35	0.87	0.90	0.21	0.80	0.90	0.17	0.89	0.87	0.36	0.88
MODEL 3	0.91	0.33	0.89	0.91	0.19	0.81	0.92	0.15	0.91	0.89	0.33	0.89
MODEL 4	0.91	0.34	0.88	0.91	0.19	0.81	0.91	0.16	0.90	0.88	0.35	0.88
MODEL 5	0.91	0.34	0.88	0.90	0.20	0.79	0.91	0.16	0.90	0.88	0.35	0.88
MODEL 6	0.91	0.33	0.88	0.91	0.20	0.81	0.92	0.15	0.92	0.89	0.33	0.89

Copyright © and. Published by Erciyes Energy Association

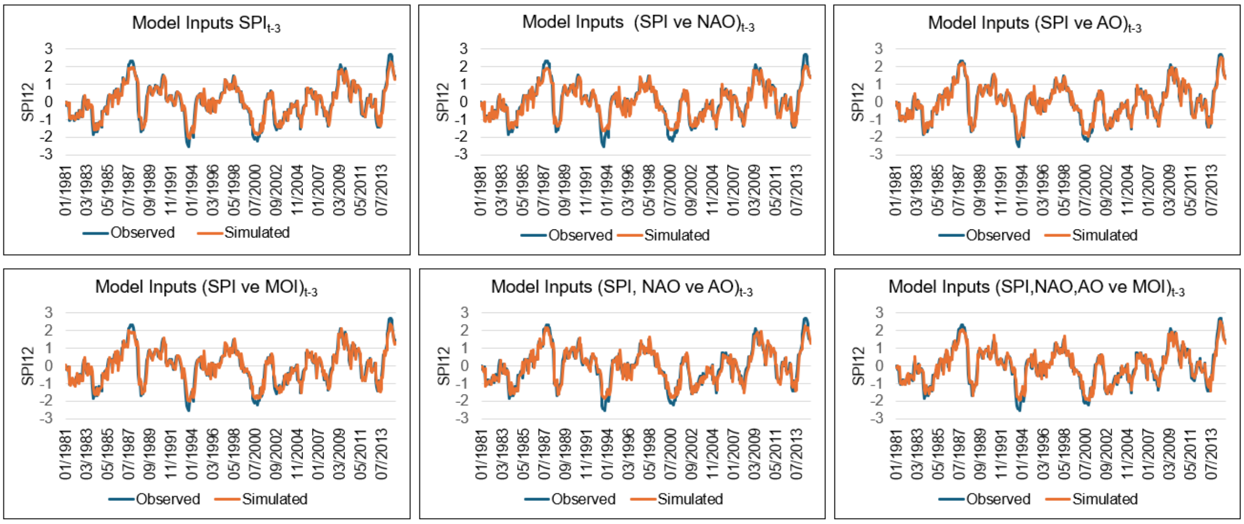

Fig. 3. Observed and Predicted SPI12 Values Based on Past 3 Months' SPI12, NAOI, AOI, and MOI1 Data

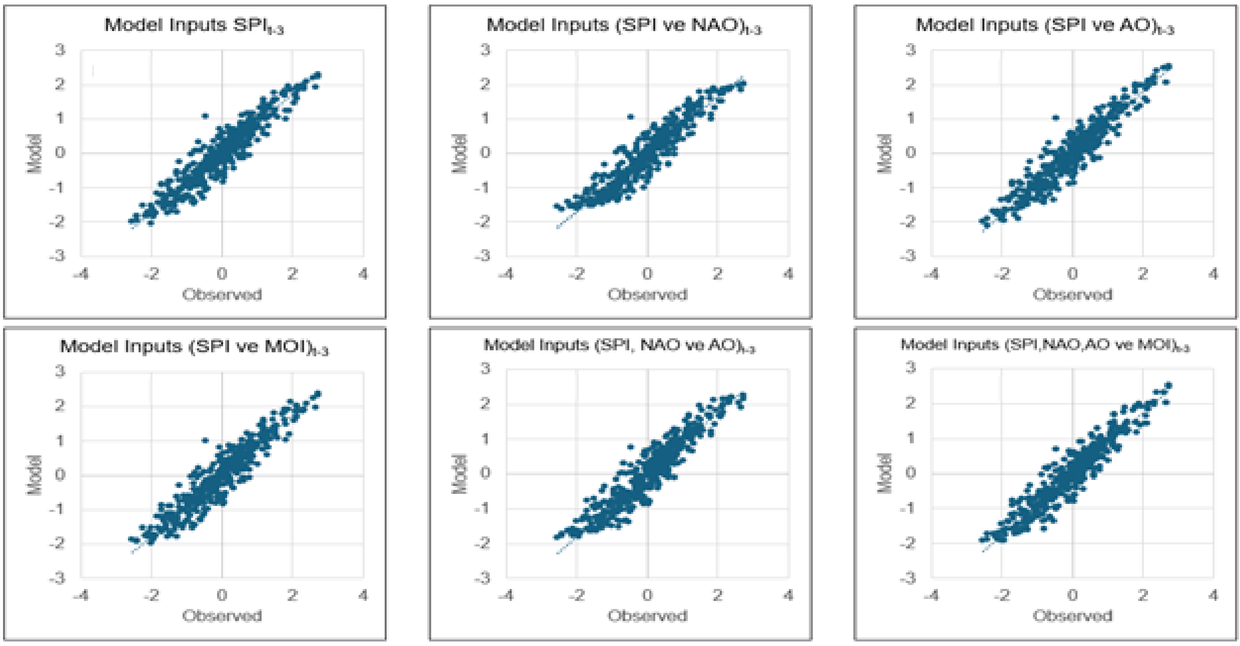

Fig. 4. Correlation of Predicted and Observed SPI12 Values Based on Past 3 Months' SPI12, NAOI, AOI, and MOI1 Data

3.3. SPI12 Forecasting Using Data from the Past 6 Months

In the second part of the study, SPI12 values were estimated using the SPI12, NAOI, AOI, and MOI1 values of the previous 6 months (Models 7 to 12). Fig. 5 and Fig. 6 present the results obtained by estimating SPI12 with different inputs. The correlation analyses of the calculated NSE, RMSE, and R^2 values are presented in Table 3.

When data from the past six months was used as input, the models that provided the best results were Models 9 and 12. In Model 9, SPI12 values were estimated using SPI12 and AOI values from the past six months. Model 12 shows the SPI12, NAOI, AOI, and MOI1 values from the previous 6. In Model 9, the NSE value was 0.90, the R^2 value was 0.90, and the RMSE value was 0.33, whereas in Model 12, the NSE value was 0.91. The R^2 value was 0.92, and the RMSE value was 0.30. The best model performance was attained when the hyperbolic tangent was selected as the activation function in the hidden layer and identity was used in the output layer.

Table 3. SPI12 Estimated Performance Evaluation Based on Past 6 Months' Data

Model No	TRAIN			TEST			VALIDATION			ALL		
	NSE	RMSE	R^2	NSE	RMSE	R^2	NSE	RMSE	R^2	NSE	RMSE	R^2
MODEL 7	0.91	0.34	0.88	0.92	0.19	0.83	0.91	0.16	0.90	0.89	0.33	0.89
MODEL 8	0.92	0.32	0.89	0.93	0.18	0.85	0.92	0.16	0.90	0.88	0.32	0.87
MODEL 9	0.92	0.31	0.90	0.91	0.20	0.81	0.92	0.15	0.92	0.90	0.33	0.90
MODEL 10	0.91	0.34	0.88	0.92	0.19	0.83	0.91	0.16	0.90	0.89	0.34	0.89
MODEL 11	0.86	0.42	0.82	0.89	0.22	0.78	0.87	0.20	0.86	0.83	0.41	0.83
MODEL 12	0.93	0.3	0.90	0.93	0.17	0.86	0.95	0.12	0.94	0.91	0.30	0.92

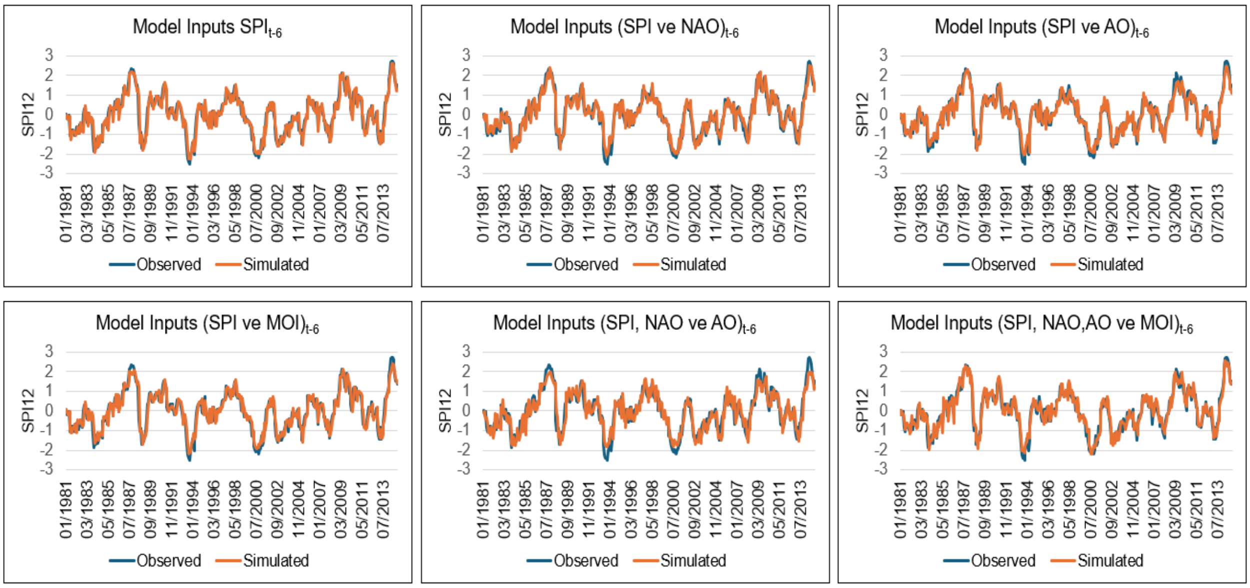

Fig. 5. Observed and Predicted SPI12 Values Based on Past 6 Months' SPI12, NAOI, AOI, and MOI1 Data

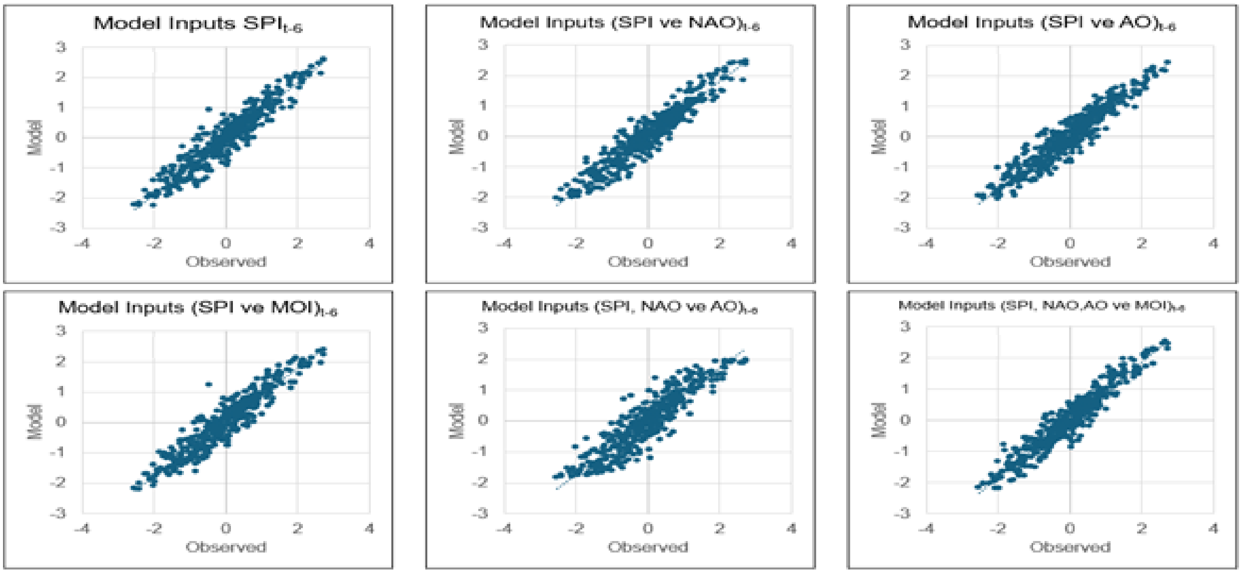

Fig. 6. Correlation of Predicted and Observed SPI12 Values Based on Past 6 Months' SPI12, NAOI, AOI, and MOI1 Data

Copyright © and. Published by Erciyes Energy Association

3.4. SPI12 Forecasting Using Data from the Past 12 Months

In the final part of the study. SPI12 values were predicted using SPI12, NAOI, AOI, and MOI1 data from the past 12 months (Models 13 to 18 in Table 1). The results obtained from predicting SPI12 with different inputs are shown in Figures 7 and 8. The calculated NSE, RMSE, and R2 values are presented in Table 4.

The best-performing models were Models 14 and 15, when data from the past 12 months was used. In Model 14, SPI12 values were predicted using SPI12 and NAOI12 values from the past 12 months. In Model 15, SPI12 values were predicted using SPI12 and NAOI. MOI and AOI values over the past 12 months. In Model 14, the NSE value was 0.91, the R^2 value was 0.91 and the RMSE value was 0.31, while in Model 15. The NSE, R^2, and RMSE values were 0.90, 0.89, and 0.33, respectively.

Table 4. SPI12 Estimated Performance Evaluation Based on Past 12 Months' Data

	TRAIN			TEST			VALIDATION			ALL		
	NSE	RMSE	R^2	NSE	RMSE	R^2	NSE	RMSE	R^2	NSE	RMSE	R^2
MODEL 13	0.92	0.32	0.89	0.92	0.19	0.83	0.91	0.18	0.90	0.89	0.33	0.89
MODEL 14	0.93	0.30	0.91	0.92	0.19	0.84	0.93	0.15	0.92	0.91	0.31	0.91
MODEL 15	0.91	0.34	0.88	0.93	0.18	0.85	0.93	0.15	0.92	0.90	0.33	0.89
MODEL 16	0.91	0.34	0.88	0.92	0.19	0.83	0.89	0.18	0.88	0.88	0.34	0.88
MODEL 17	0.90	0.35	0.87	0.91	0.20	0.83	0.91	0.16	0.90	0.88	0.35	0.88
MODEL 18	0.89	0.37	0.85	0.91	0.19	0.82	0.90	0.17	0.89	0.87	0.37	0.87

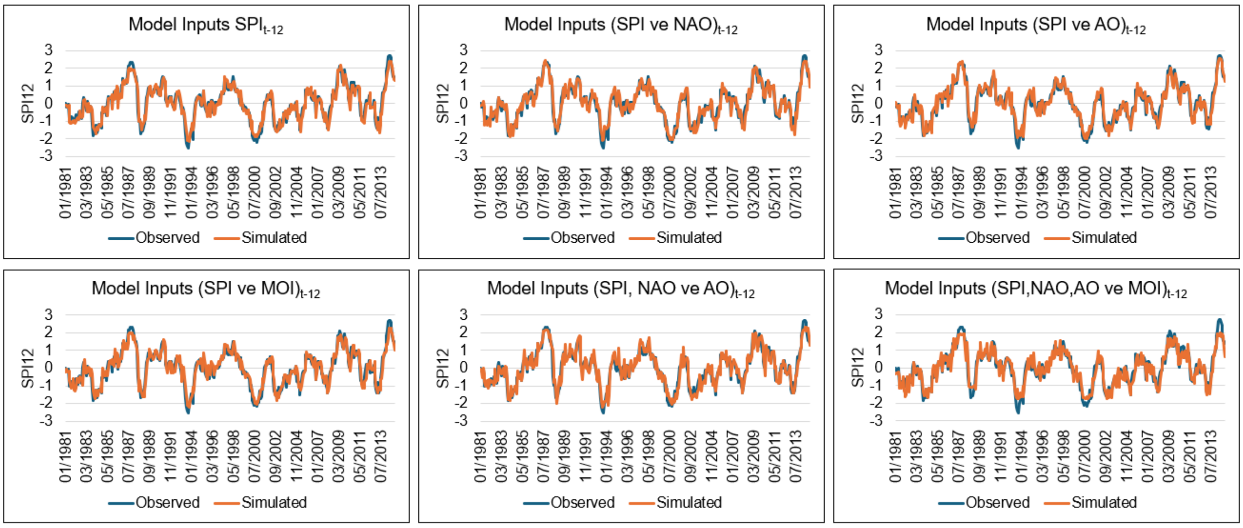

Fig. 7. Observed and Predicted SPI12 Values Based on Past 12 Months' SPI12, NAOI, AOI, and MOI1 Data

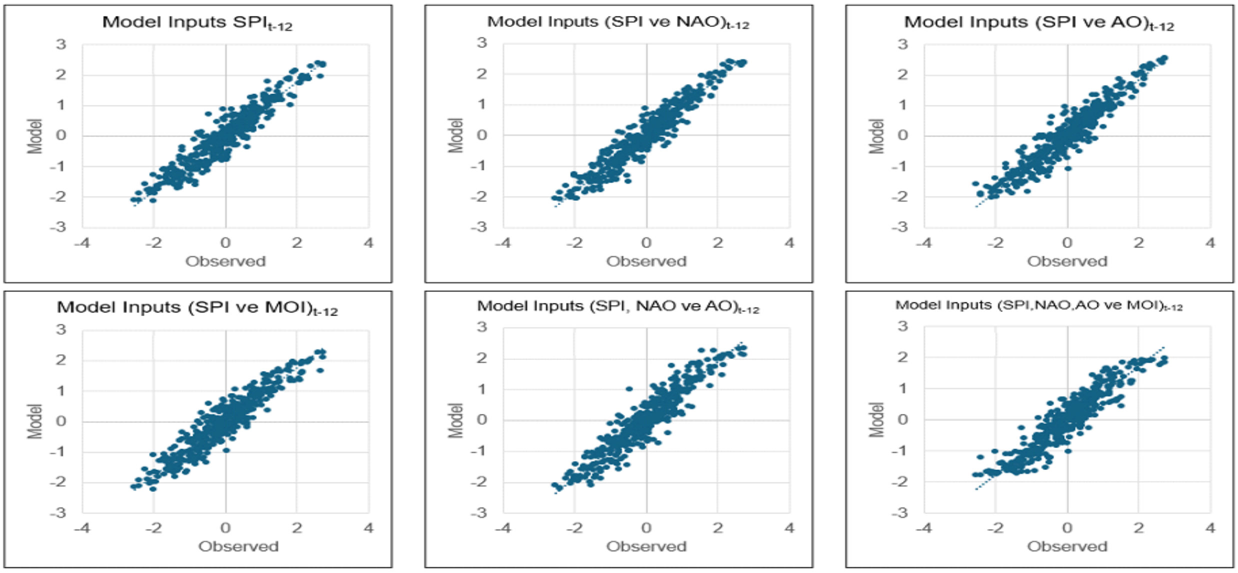

Fig. 8. Correlation of Predicted and Observed SPI12 Values Based on Past 12 Months' SPI12, NAOI, AOI, and MOI1 Data

4. DISCUSSIONS AND CONCLUSION

This study aimed to develop and apply robust and accurate models for drought prediction. Given the complexity and challenges of drought forecasting, it is essential to employ various approaches to capture the nonlinear relationships between drought and meteorological variables. Numerous climatic factors contribute to the occurrence of droughts. The objective was to identify the most effective model or technique for predicting drought under future climate scenarios.

This study developed an ANN model to predict the Standardized Precipitation Index at a 12-month scale (SPI12) using large-scale global climate indices. An Artificial Neural Network (ANN) technique was employed as the modeling approach. The model performance was evaluated using RMSE, R^2, and NSE metrics. In the developed models, SPI12 was used as the dependent variable, while the independent variables included lagged values of SPI12, AOI, NAOI, and MOI1 from the preceding 3, 6, and 12 months.

As a result of the modelling studies, the RMSE values of the SPI12 prediction models ranged from 0.30 to 0.41. The R^2 values ranged from 0.83 to 0.92, and the NSE values ranged from 0.83 to 0.91. The best performance was achieved by Model 12, where the RMSE, $R^{2,}$ and NSE values were 0.30, 0.92, and 0.91, respectively. This result shows that the best prediction performance was obtained when SPI12, NAOI, AOI, and MOI1 values from the preceding six months were used together.

In this study, the ANN method was chosen as the modeling technique. An ANN is a data-driven model that can be used to model complex systems. This method has been used in many studies for SPI prediction [e.g., 13, 14,15]. In this study, using precipitation data, SPI12 values, and large-scale oscillation index data as inputs, the model predicted the SPI12 value with an R^2 value of 0.92 and an RMSE value of 0.30. Similarly, Morid et al. [17] developed a model based on SPI inputs and index values and achieved an R^2 in the range of 0.66-0.79 based on data from the preceding 6 months. Rezaeian-Zadeh [18], incorporating antecedent SPI, precipitation, and both the North Atlantic Oscillation and Southern Oscillation Index, achieved the highest forecasting performance, with an R^2 of 0.92 and an RMSE of 0.35 for 1-month lead time predictions during the validation phase. The performance metric values obtained in this study closely approximate those reported in the literature in magnitude and are at an acceptable level.

This study revealed that large-scale global oscillation indices influence precipitation patterns in Kayseri, and in this sense, the findings agreed with those of the previous studies. The effects of global oscillation indices on precipitation and drought in Türkiye have been demonstrated in previous studies [3, 4, 5, 6, 7, 8, 9, 10, 11] Karabörk et al. [4] analyzed the variability of climate variables in Türkiye based on the Southern Oscillation Index (SOI) and NAOI and showed that NAOI affects precipitation and runoff during winter months. Topuz et al. [10] analyzed annual and seasonal precipitation data from 29 stations in Türkiye between 1955 and 2013. The effect of atmospheric circulation on precipitation variability in Türkiye was investigated using NAOI, MCI, MOI, EMPI, and NCPI. As a result, it was found that the MOI better explained annual precipitation variability in Türkiye than the other indices. Duzenli et al. [9] showed in their study that the NAOI and AOI affect the dry days in all regions of Türkiye, except for the east and northeast during the winter months. Furthermore, when comparing the effects of large-scale global oscillation indices on precipitation extremes and dry days, it was concluded that large-scale global indices significantly impacted the number of dry days. Dadaser-Celik et al. [11], using data from 238 meteorological stations in Türkiye, also showed that large-scale global oscillation indices significantly influence Türkiye's precipitation patterns, and these effects are observed both annually and seasonally.

This study distinguished the potential of predicting SPI using climate indices, precipitation data, and artificial intelligence techniques. It was suggested that new models

Copyright © and. Published by Erciyes Energy Association

and scenarios could be developed by adding new data in future studies, and the performance indicators could be improved using such algorithms as deep learning.

REFERENCES

[1] A. Zargar, R. Sadiq, B. Naser. A Review of Drought Indices. *Environmental Reviews*, Vol. 19, pp. 333-349, 2011.

[2] T. B. McKee, N. J. Doesken, J. Kleist, J. The Relationship of Drought Frequency and Duration to Time Scales. In Proceedings of the 8th Conference on Applied Climatology, Anaheim, 1993.

[3] F. K. Sönmez, A. Ü. Kömüşcü., A. Erkan. E. Turgu. An Analysis of Spatial and Temporal Dimension of Drought Vulnerability in Turkey Using the Standardized Precipitation Index. *Natural Hazards*. Vol. 35(2), pp. 243-264, 2005.

[4] M. Ç. Karabörk, E. Kahya, M. Karaca. The Influences of the Southern and North Atlantic Oscillations on Climatic Surface Variables in Turkey. *Hydrological Processes*. Vol. 19(6), pp. 1185-1211, 2005.

[5] M. Türkeş. E. Erlat.. Influence of the Arctic Oscillation on the Variability of Winter Mean Temperatures in Turkey. *Theoretical and Applied Climatology*. Vol. 92(1), pp. 75-85, 2008.

[6] M. Türkeş. E. Erlat. E. Winter Mean Temperature Variability in Turkey Associated with the North Atlantic Oscillation. *Meteorology and Atmospheric Physics*. Vol. 105, pp. 211-225, 2009.

[7] İ. Sönmez, A. Ü. Kömüşcü. Reclassification of rainfall regions of Turkey by K-means methodology and their temporal variability in relation to North Atlantic Oscillation (NAO). *Theoretical and Applied Climatology*. Vol. 106, pp. 499–510, 2011.

[8] A. Karakoç, Ş. Tağıl. İzmir ve Ankara'da Yağış Paterni ile Kuzey Atlantik Salınımı (NAO) Arasındaki İlişki. Journal of International Social Research. Vol. 7(30), pp. 148-157, 2014.

[9] E. Duzenli. H. Tabari, P. Willems. M.T. Yilmaz. Decadal Variability Analysis of Extreme Precipitation in Turkey and Its Relationship with Teleconnection Patterns. *Hydrological Processes*. Vol. 32(23), pp. 3513-3528, 2018.

[10] M. Topuz, H. Feidas, M. Karabulut. Türkiye'de Yağış Eğilimleri (1955-2013) ve Atmosferik Dolaşım. *Tücaum*. Vol. 30, pp. 3-6, 2018.

[11] F. Dadaşer-Çelik, Ö. Karadeniz, A.Ü. Kömüşcü, M. Çelik. Relationships Between Large-Scale Atmospheric Teleconnection Indices and Precipitation Over Turkey from 1980 to 2015. 9th International Symposium on Atmospheric Sciences (ATMOS 2019), İstanbul, 2019.

[12] E. Servat, A. Dezetter. A. Selection of Calibration Objective Functions in the Context of Rainfall-Runoff Modeling in a Sudanese Savannah Area. *Hydrological Sciences Journal*.Vol. 36(4), pp. 307-330, 1991.

[13] S. Sırdaş, Z. Şen. Meteorolojik Kuraklık Modellemesi ve Türkiye Uygulaması. *İTÜ Dergisi*. Vol. 2(2), pp. 95-103, 2003.

[14] A. Malik, A. Kumar, P. Rai, A. Kuriqi. Prediction of Multi-Scalar Standardized Precipitation Index by Using Artificial Intelligence and Regression Models. *Climate*, Vol. 9, pp. 28, 2021

[15] F. B.Banadkooki, V. P. Singh, M. Ehteram. Multi-timescale drought prediction using new hybrid artificial neural network models. *Natural Hazards* 106, 2461–2478, 2021.

[16]. V. Gümüş, A. Başak, K. Yenigün. Yapay Sinir Ağları ile Şanlıurfa İstasyonunun Kuraklığının Tahmini. *Gazi Üniversitesi Fen Bilimleri Dergisi Part C: Tasarım ve Teknoloji*. Vol. 6(3), pp. 621-633, 2018.

[17] S. Morid, V. Smakhtin, K. Bagherzadeh.. Drought forecasting using Artificial Neural Networks and time series of drought indices. *International Journal of Climatology*. Vol. 27, pp. 2103-2111.

[18] M. Rezaeian-Zadeh, H. Tabari. MLP-based drought forecasting in different climatic regions. *Theoratical Applied Climatology*. Vol. 109, pp. 407–414, 2012.